Modelling and measurement of ultrasound vibration potential distribution in an agar phantom

Fria Hossein[a] and Mi Wang[b]

School of Chemical and Processes Engineering, University of Leeds, UK

[a]Email: py12fah@leeds.ac.uk [b]Email: m.wang@leeds.ac.uk.

Abstract

Ultrasound vibration potential (UVP) is an electric signal generated from the vibration of particles or ions along with the trajectory of the ultrasound pulses travelling through a colloidal suspension or ionic electrolyte. Therefore, it may be used to characterize or image the physiochemical property of particles or ions. This paper presents a modelling method based on the principle of static charged disc dipole and its equivalent circuit to model the ultrasound vibration potential distribution (UVPD) inside domains of interest. A tissue-like testing phantom (in 82×56×66 mm) embedded with one or more sample cells made from either agar or colloids with two electrodes fitted at optimized locations outside of the phantom is reported. The UVP measurements in peak-to-peak amplitude of 162/309 μV and 419/499 μV are measured from two interfaces of a single cell setting with either KCL (1 M) or nanoparticles (SiO2 in 21 nm, 1wt %) agar gels respectively. Results from the measurement comply with the modelling of UVPD, which are evidenced from UVP measurements of a setting up with six interfaces of three cells, demonstrating the feasibility of using the static electricity modelling method to estimate UVPD.

Keywords

Ultrasound vibration potential distribution, modelling, static charged disc dipole, measurement, nanoparticles, ionic species agar phantom.

1 Introduction

The concept of ultrasound vibration potential (UVP) (also called ion vibration potential - IVP) for ionic electrolytes dates back to Debye [1]. He realized that an electric signal is generated in electrolytes upon the introduction of ultrasound pressure. Several works have been published to reveal and explore this phenomenon. Particularly, the expressions based on ion vibration potential and based on colloid vibration potential (CVP) given by Ohshima and Dukhin [2] and O'Brien [5], respectively. Many experimental works were also conducted to validate above models and/or to evaluate the potential of UVP for imaging in medical and engineering applications, with either a vertical or a horizontal water phantom with metal wires or mesh electrodes, including responses from physiochemical properties of ionic species or nano-particles in colloids [3, 4, 6, 8, 9]. UVP experiments of soft tissue and blood are firstly, muscle tissues from chicken breast, beef, and pork all produced vibration potentials with smaller than 0.02 μV while whole blood gave comparatively larger signal 10μV, and UVP two dimensional imaging of thin layer silica colloidal disks was cast in agarose reported by reported by Andrew et al., [11]. Recently, we have demonstrated specific physiochemical structures of animal tissue (pork) can be revealed by UVP, in comparison of signals from conventional ultrasound, which the conventional ultrasound technique cannot be seen [10]. Several works on understanding of ultrasound vibration potential distribution (UVPD) were reported. Gusev and Diebold presented the general form of UVPD in an infinitive space and in a slab model with two parallel ground electrodes [3]. Wang et al [8] also expressed an extended 2D slab model and a 3D dipole model to address the forms of potential measurements in relation to periods of ultrasound pulses and composition of the medium. Further, Cuong et al [7] derived UVPD in the slab model for colloidal infinite layers, upright cylinders, and spheres based on recording current from a time varying polarization. The above models present a good knowledge for understanding of the principle and mechanics of UVPD but with a level of complexity in practise. In this paper, we present a numerical simulation based on the principle of static charged disc dipole and its equivalent circuit to model UVPD inside a finite domain of interests. A tissue-like testing phantom embedded with one or more sample cells made from agar and two electrodes fitted at optimized locations at the outside of the phantom. Cross evaluations between modelling and measurement are reported.

2 Ultrasound vibration potential distribution (UVPD)

2.1 Disc dipole model

It is understood that an alternating electric field will be generated by polarisation of charged ions/particles and their counter ions along the ultrasound pulse propagation inside electrolyte or

colloid. The electric field is function of electric field as a function of ultrasound propagation in time and space. Wang et al [8] suggested that the polarisation might be considered as it's generated by number of dipoles along an ultrasound travel path. The measurement of UVP is an integration between two points across a space of the electric field at a specific time. UVP measured over a time window may present a waveform having the same frequency and similar pulsation as the pulsed ultrasound. Therefore, one static charged disc dipole at a specific location may be adopted to model the UVPD generated by ultrasound pulse travels through a specific location (an interface of a slab) over a time. Concerning the effect of ultrasound beam width, a disc shape of the dipole is proposed. Due to the effect of integration, the minimum thickness of the slab should be at least greater than the wavelength of the ultrasound. In order to enhance the signal-to-noise ratio, more than one pulse of ultrasound are used to distinguish the interface of the slab, which was addressed by Diebold et al [11] and Wang et al [8]. Under this, assumptions that attenuations of ultrasound propagation and electric field distribution over a distance in few wavelengths of the ultrasound pulses are ignorable. The ions or particles in medium are in uniform distribution, the UVP measured between two points over an interface of two species of ions/particles may not be a nonzero value if the specific physiochemical properties of species are not the same or zero if the species are the same. The polarity of the UVP is also determined by the physiochemical properties of species. Then, UVP and its distribution UVPD may be concerned as they are generated by ONE static charged disc dipole located at the interface of a sample cell due to temporal steady state of ultrasound pulses in their propagation cross the interface. UVPD always refers to a zero-potential plane between the dipole orthogonal to the direction of ultrasound propagation. The diameter of charged discs is set at the same size as the ultrasound beam width. The distance between two discs is set as the same length as the wavelength of the ultrasound in agar. The beam propagation is uniformed and planar. The effects of wave attenuation, divergence, etc. are ignorable.

To solve the potential distribution, we use COMSOL Multiphysics to create a numerical model. Figure 1 illustrates the model setup. The medium block has finite dimensions [$\text{width} = 82\ \text{mm}, \text{depth} = 56\ \text{mm}, \text{height} = 66\ \text{mm}$] with physical properties of conductivity = 0.0136 S/m, relative permittivity = 81.5 and temperature = 293.15 K. The two-disc dipoles are set with silica dielectric properties and zero conductivity, positioned in parallel with a diameter of 25 mm and placed at the centre of the medium block. The separation distance between the canters of the two discs is 1.6 mm and the thickness of each disc is 0.2 mm. The charges set to discs are +/- 1 C, respectively. In the model, the coordinate of the central planar plane along the ultrasound propagation direction between both dipoles is zero. Two measurement electrodes are located at the far corners of the nearside and rear-side of the medium block for the convenience in the experimental setup. A grounding ring at the nearside is also included to model the

grounding contact between the metal shell of ultrasound transducer and the medium block in the experimental setup. The thickness of the slab should be greater than the multiple wavelength of the ultrasound in order to use more than one pulse of ultrasound to distinguish the interface of the slab. A static electric field (or DC field) is used to describe the potential distribution in an agar region. In Figure 1 we have used only one disk dipole in the model. This to model the UVPD generated from the integration, which does not directly refer to the dipoles along the path of ultrasound.

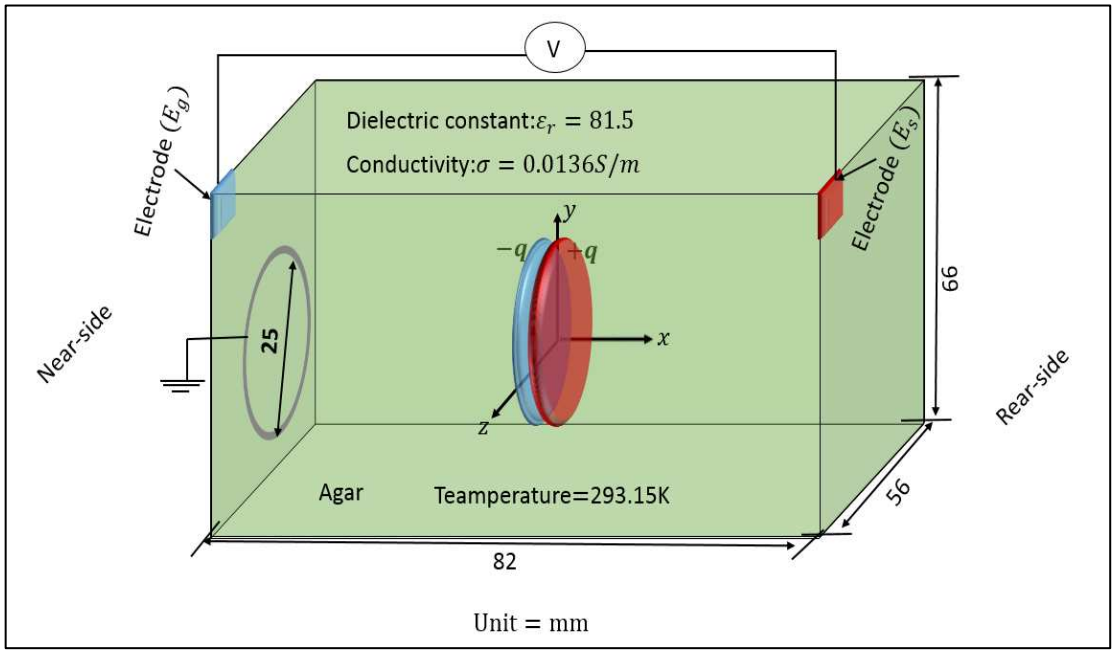

Figure 1: Diagram of disc dipole model

2.2 Equivalent circuit

The UVP signal is generated at the interface between the sample cell and the medium where physiochemical difference exists, which is presented with an equivalent circuit diagram as shown in Figure 2. The static current, I, is induced by the ultrasound pulses. Ultrasound excitation voltage is applied between two electrodes, E_g and E_s; and bulk impedance of the medium is denoted as Z. Since the zero current through the voltage meter is assumed, the effects of electrode-electrolyte interface [4] can be ignored.

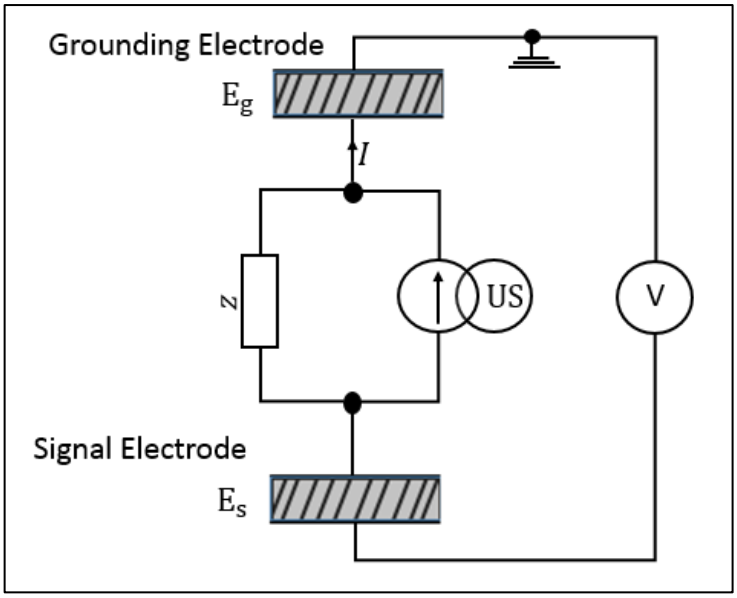

Figure 2: The equivalent circuit diagram of the UVP generation and detection.

2.3 Potential distribution

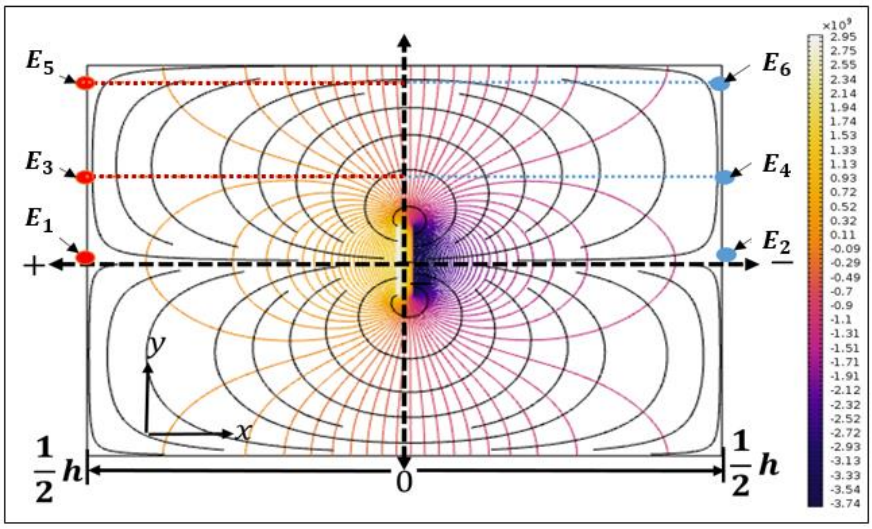

Figure 3: Simulated ultrasound vibration potential distribution at the central cross section of the medium block– equipotential lines are coloured, and current streamlines are in black.

Figure 3 shows the simulated potential distribution at the vertical cross-section of the medium block, where the ultrasound is propagating from the left to right along the centre of the block and the cross-section. Due to the symmetrical nature of UVPD presented in the simulation, only data in the half of the cross-section is reported. The coloured lines represent the equipotential lines, and the black lines represent the current streamlines. In the figure 3, the origin of the coordinate is set at the centre between the two charged discs. It is also as expected, that the potential over the plane between the two discs in the dipole is zero. The results show that the

UVP is better to be measured between the nearside and rear-side (see Figure 1) of the phantom and maximum value can be obtained between the two points along the propagation direction.

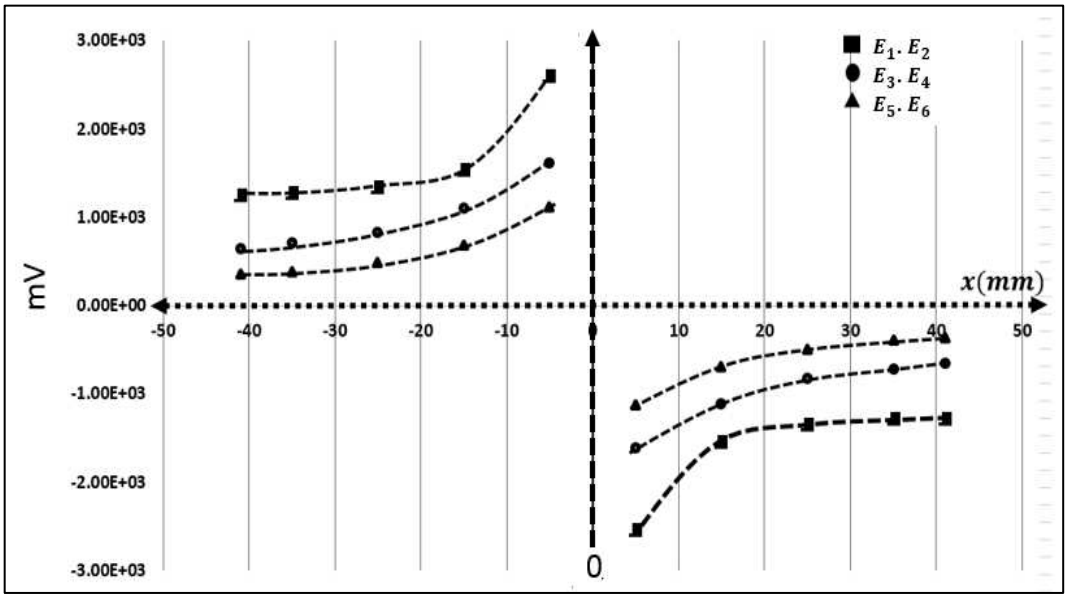

Figure 4: Simulated UPVD inside the medium block along E1 (0.1, 28) andE2 (81.9, 28) and E3 (0.1, 38) and E4 (81.9, 38) and E5 (0.1, 48) and E6 (81.9, 48), respectively.

Figure 4 shows the potential distribution across the finite region of the model contains a disc dipole. The UVPD were simulated with electrodes placed at different locations. It is worth to notify all UVPD in Figure 4 are referred to zero potential plane. The potentials along the E1 and E2 are larger than the potentials along E3-E4 and E5-E6, respectively. The electric potential increases when the test point is closer to the source of charged discs, and it is inversely proportional to the distance between the test point and the source of charge. The maximum potential can be measured when the test points are set along the axis of the ultrasound propagation direction.

The beam width of ultrasound in its propagation may have significant effects on the strength of signal and format of attenuation in the medium block. These effects were investigated by presenting disc dipole in different sizes, where the materials and the total charge of these setups were kept the same as stated in the previous section. UVP measured between two electrodes (Es-Eg), placed at (0.1, 28), and (81.9, 28) respectively. We relocated the positions of the disc dipoles inside the body in the x-direction from left to right and represent in (x,) plane. The disc dipoles positioned at six different locations at [(14, 16), (22, 24), (36,38), (44, 46), (58, 60), (66, 68)] mm inside the agar block. The results are presented in Figure 5 as the function of the

diameter of charged discs. It is noted that the potential intensity increases with the decrement of disc's diameter, and potential uniformity improves with the increment of disc's diameter.

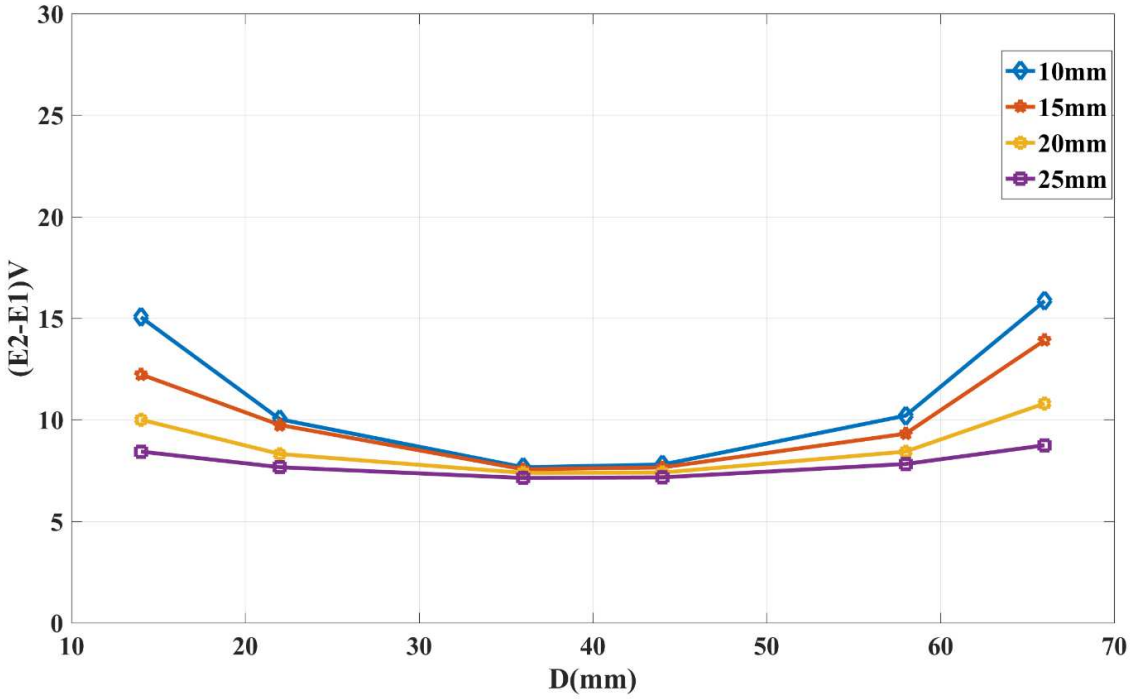

Figure 5: UVP measurement from the disc dipole model with charged discs in diameter of (R=10, R=15, R=20, R=25) mm, respectively.

3 UVP measurement

3.1 Materials and methods

Electrolytes and colloids:

Potassium Chloride (KCL, 99% purity) was purchased from Sigma Aldrich (UK). The sample in 1M concentration was prepared by dissolving 7.455g of KCL in 100ml deionized water. The colloidal suspension of Silica Nanoparticle ($\mathbf{SiO_2}$) was purchased from Fuso Chemical CO, Ltd, Japan. The sample size provided by the manufacturer was 12 nm. The sample was firstly weighted up using a balance, de-ionised process using an ion exchange resin beads (Bio-red) and then diluted to 1wt% concentration. It is understood that the particle size may change due to the aggregation and pre-treatment process. Therefore, particle size distribution was measured after preparation using Malvern Zeta Sizer. Malvern Zeta Sizer is based on the principle of electroacoustic effect of charging particles in colloids, which takes an assumption of particle in spherical shape. The sample was first weighed using a balance accurate to 2 decimal places and the original sample was deionized using ion exchange resin beads (from Bio-Rad) and diluted to 1 wt% concentration. The nominal size measured with Zeta Sizer was 21nm.

Mock body and sample preparation

Agar gel as one of tissue-mimicking materials is widely used in many ultrasound studies to research phenomena invitro and predict in-vivo bio-effects [12], which can form a phantom with a good mechanical strength even in 1 wt% concentration. Agar consists of a mixture of two polysaccharides: agarose and agaropectin, with agarose making up to 70% of the mixture. The agar powder was purchased from Special Ingredients Ltd. (UK). To prepare a mock body, 1wt% agar gel, 500 ml of de-ionised water were heated to 85 ℃ before introducing the agar powder in a large beaker. Then 5g of agar powder was added to the beaker mixed with a magnetic stirrer inside. The solution was then continually heated up for 2 hours at a temperature of 80 ℃ to remove air bubbles. The temperature remained stable for up to 30 minutes in order to dissolve the agar completely. The suspension was then transferred to a vessel for cooling (to decrease the temperature), achieving a good firm block of agar, and left overnight to cool. The cubic shape of palustrine material with dimensions of 10 mm in thickness, 30 mm in length and 40 mm in depth was placed (inserted) the agar gel before it cools down to make a space for the cell. Following the similar procedure, the test samples were prepared with nanoparticle colloids to make the single sample cell. To avoid a 'hard interface' between the sample cell and the agar medium and to make the interface 'invisible' (with no reflection of the ultrasound), the sample was introduced to the mock body at a temperature of 85 ℃ and left overnight to cool.

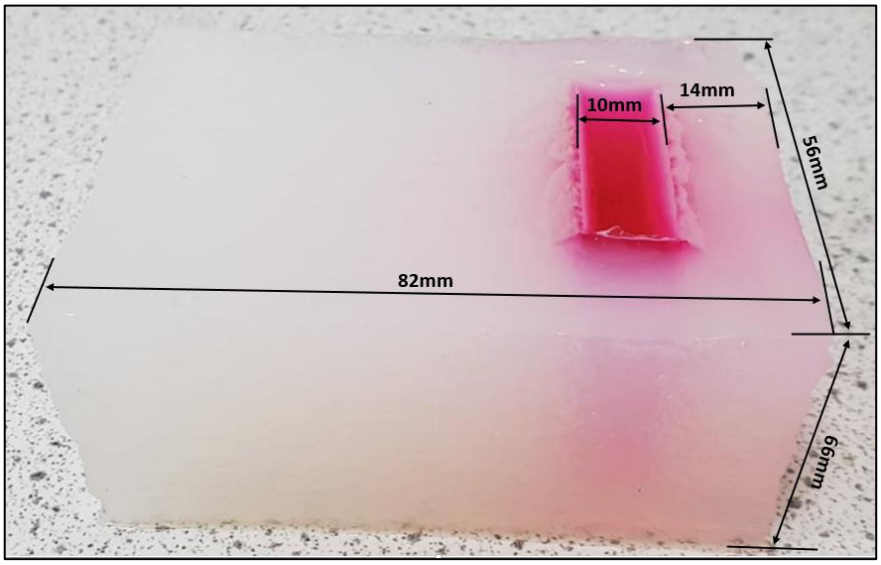

Figure 6: Agar Mock Body.

Figure 6 shows the mock agar body in white colour and a cell (without specified ions or particles) in red colour.

In multi-cell experiment (section 3.4), the nanoparticle suspension directly introduced into the cells without avoiding hard interfaces as shown in Figure 10. These results in a larger signal

amplitude compared to the single cell experiment because of the enhanced mobility of nanoparticles in solution. In the single cell experiment, particles mixed with agar and the sample cell forms a gel. These results in a weaker vibration compared to the multi-cell experiment, where the sample is not mixed with agar powder.

3.2 Experiment and sensor set-up

The set-up consists of two parts: the excitation and measurement. The excitation includes the signal generator (Model 33250A manufactured in 2016) with an set-up of 450 mV (pk-pk) amplitude, 1 MHz , frequency and six duty cycles over a burst period of 50 ms, providing a duty cycle of 0.01%. The signal generated from the signal generator is send to the RF amplifier (Model GA-2500A manufactured in 2016) for amplification. The excitation signal is amplified by 40 dB. The output from the RF amplifier is coupled with an impedance matching resistor in**50 Ω.** Then it connected to the 1 MHz piezoelectric transducer in a diameter of 25 mm and fixed at the near side of the agar block. This transducer converts the electric signal to a mechanical pressure wave or ultrasound. The measurement for this experiment consists of two electrodes made from aluminium foil having a square shape with dimensions 10 × 10 mm. The UVP signal detected by both electrodes. The signal amplified with a voltage amplifier (Model 5072PR manufactured in 2015) with an amplification factor of 39 dB, and then sent to the digital LeCroy oscilloscope (Model 2GS/s DSO manufactured in 2004) averaged over 256 times for calibration and data collection. The diagram of the experimental setup is presented in Figure 7.

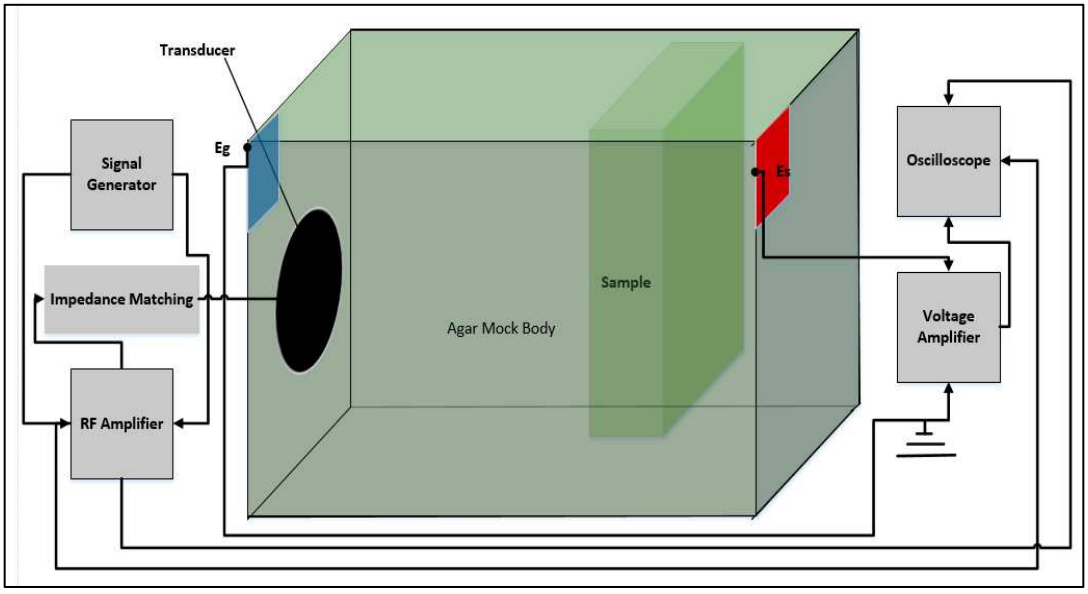

Figure 7: Diagram of experimental setup

3.3 UVP signal strength with an agar body.

Colloid vibration potential (CVP) signal

The colloidal sample used for the CVP test was silica dioxide (SiO_2) with a particle size of 21 nm and concentration of 1wt%. The sample was embedded into the agar block at a position 58 mm away from the transducer interface. The colloidal sample cell is in dimension of x = 10, y = 30, and z = 40 mm. The zoomed two bursts of CVP signal generated from two interfaces of the sample cell are shown in Figure 8. The two bursts of CVP signal have a 180° phase shift between them, reporting the different value of UVP between those from the medium or the 3 samples. The CVP signal was measured as 419 $\mu V_{(pk-pk)}$ for the first pulse A1 and as 499 $\mu V_{(pk-pk)}$ for the second pulse A2, where A1 is the UVP signal appeared at the first boundary of the slab and A2 is the UVP signal appeared at the second boundary of the colloidal slab towards the ultrasound transducer as the setting shown in Figure 6.

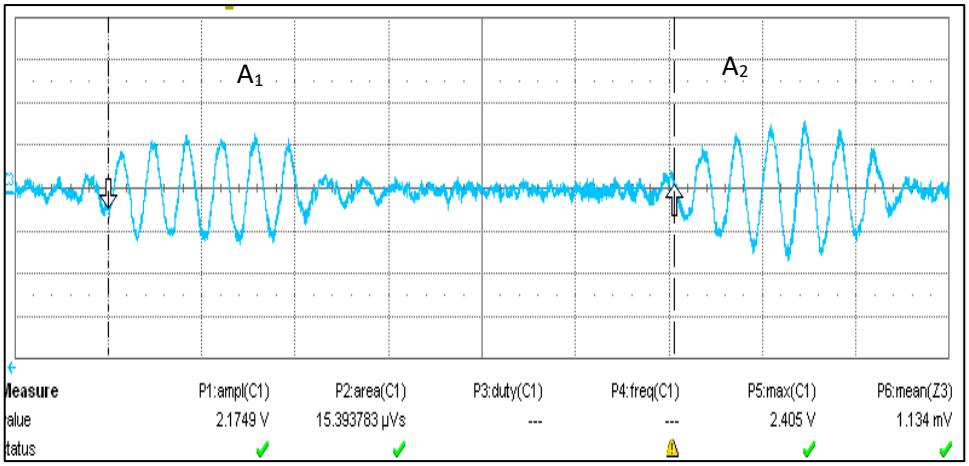

Figure 8: CVP signal with a burst of 6 cycles for silica dioxide with 21nm size and 1wt% concentration, with gain factor of 39dB.

The first burst of the CVP signal appeared at 38.2 µs from the transducer interface. The ultrasound speed measured in agar as 1600 m/s. The measured distance between the transducer interface and the first boundary of the sample given at 61.1 mm. The setting distance between the sample and the transducer interface is 58 mm, and the error is 0.5%. The second burst appeared in 44.95 µs, giving the distance from the transducer interface to the exit layer of the sample at 71.92 µs. The sample thickness was measured at 10.82 mm. The cell thickness was 10 mm, and the error of 0.8% on the sample thickness was made by the diffusion of the sample to the agar mock body. The different between the first and the second signal mainly due to the electric field attenuation, which is a function of the distance between the interface (as a source), and the electrodes (as a measurement) as discussed in the previous section. A2 is higher than

A1 in Figure 8 since the distance between the second interface and the right electrode is closer, therefore, A2 measured with less attenuation than A1.

Ion vibration potential (IVP) signal

The IVP test was carried out using KCl with a concentration of 1M. The IVP signal was measured at 309 $\mu V_{pk\text{-}pk}$ for A2. The IVP signal from the sample for the first pulse, A1, is measured at 162 $\mu V_{pk\text{-}pk}$. The two bursts of IVP signals appeared in 38.11 µs and 45.02 µs respectively for A1 and A2.

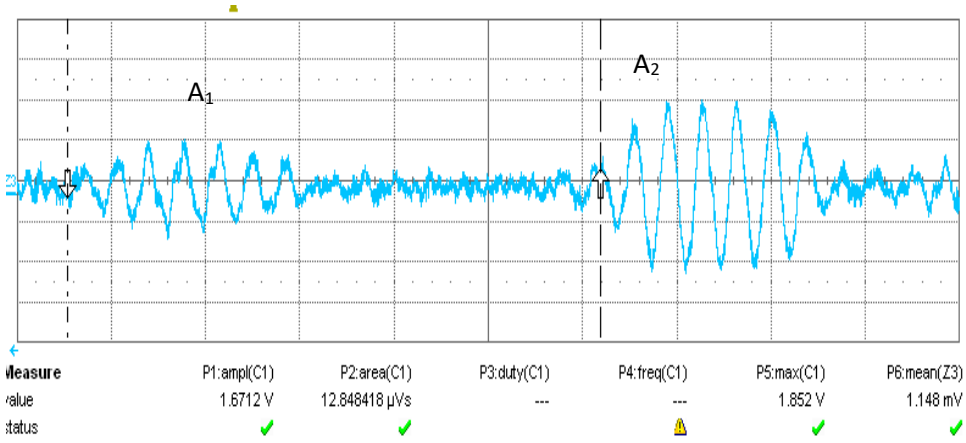

Figure 9: IVP signal with a burst of 6 cycles for KCL with the concentration of 1M, with a gain factor of 39dB.

By taking the ultrasound speed in the agar mock body as 1600 m/s, the thickness of the sample was measured at 11 mm. The 1% error due to the diffusion of the electrolyte into the agar mock body. The first signal, A1 is much weaker than the second, A2, comparing to the signal from the CVP. The shift may be due to the current bias of a voltage meter in practice, which is under a further investigation.

3.4 Model Evaluation

The agar mock body was set with three sample cells with the same silica nanoparticle suspensions and concentration as expressed previously but without agar to enhance the signal-to-noise ratio. To enhance the visibility, the suspension was dyed in green colour. The sample cells, represented in a green colour, were placed at different positions as shown in the Figure 10. Each sample cell has a dimension of width 10 mm, length 30 mm, and height 40 mm. The first sample was embedded at 14 mm away from the transducer interface or front side. The second sample was placed 36 mm away and the third sample embedded at 58 mm away from the nearside of the mock body.

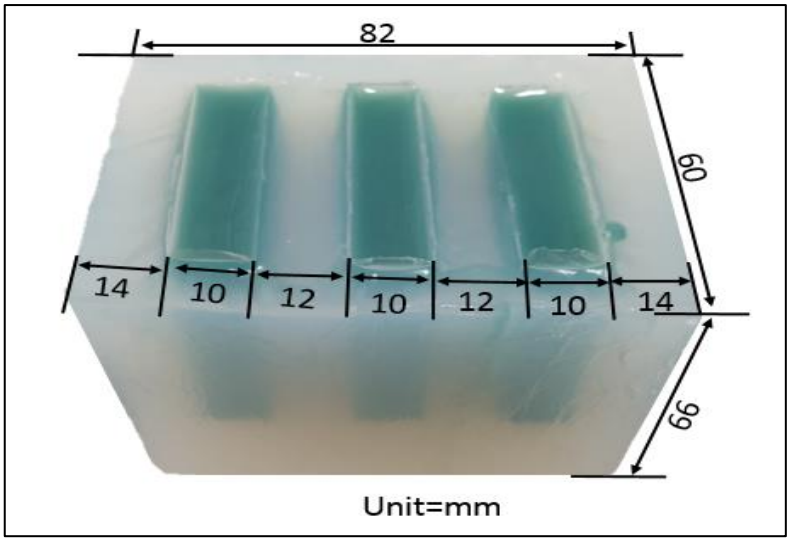

Figure 10: Agar mock body with three sample cells.

The experimental set-up was exactly the same as the diagram shown in Figure 7. The four periods of ultrasound pulses sent into the mock body of agar were via a piezoelectric transducer having a frequency of 1 MHz. The electric potential signals were generated from the interfaces between the agar medium and sample cells. The UVP signals were detected by the electrodes and amplified by the voltage amplifier with a gain factor of 39 dB. The amplified signals were displayed on the oscilloscope as shown in Figure 11.

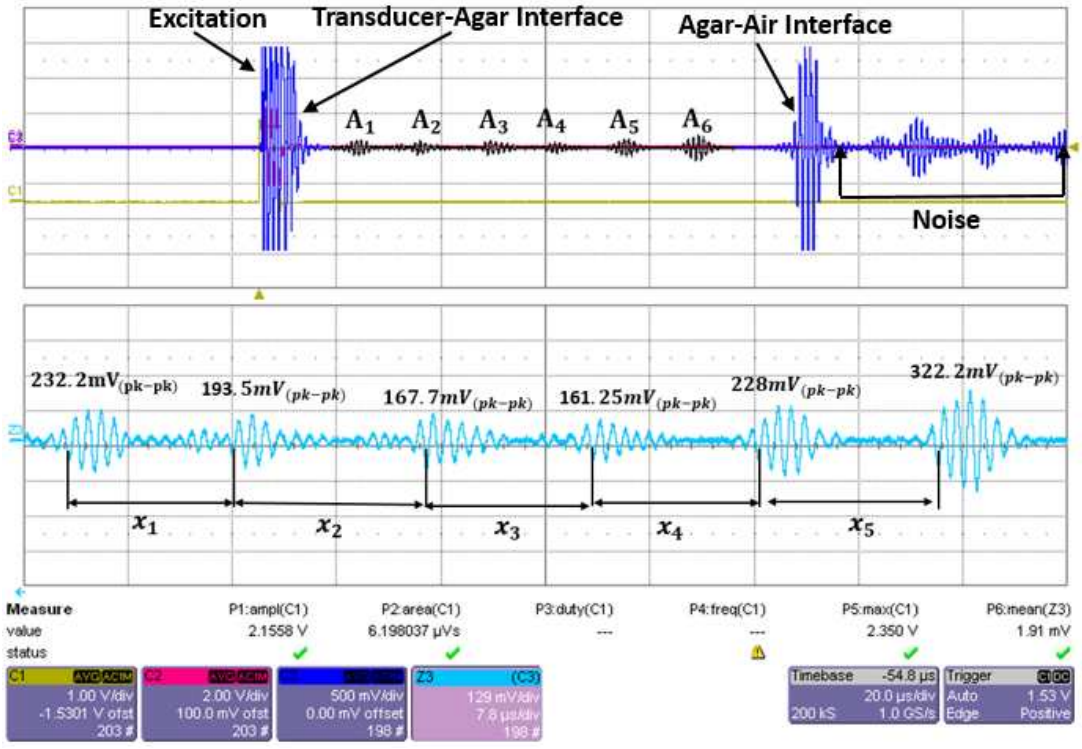

Figure 11: UVP signals (with gain 39dB) from an agar mock body containing three sample cells (SiO2, 21nm, 1wt %,) at different positions.

In Figure 11, the first group of pulses is from the electric field induced by the transducer exaction. Then, six groups of pulses, named from A1 to A6, are believed as the UVP signals generated from six interfaces of three sample cells. The last group of pulses with high intensity is from the agar-air interface at the right-end of the agar phantom. Which is believed as the plate of the end electrode (Es as illustrated in Figure 7) is at the same plate of the agar-air interface, which is also close to the source of UVP generated by the interface where the electric field has a very high intensity and sharp gradient as shown in Figure 3 and 4. The assumptions on the difference from attenuation of dipoles ignorable expressed in Section 2.1 would not be satisfied. Therefore, the signal from the agar-air interface has nonzero value and high intensity although the incident and reflected ultrasound may have similar amplitude. The UVP signal at A6 is larger than A5 and A4 but A1 is larger than A2 and A3, which are because of electric field distributions produced by the disc dipole at corresponding locations. The distance between the sample and the electrode sensor plays a major effect on the signal amplitude. The set locations of sample cells and UVP pulse positions measured in consideration of ultrasound pulse propagation. The measured CVP signals are shown in Table 1, where n denotes the order of the interface cells from nearside of the mock body, X and X' are the distance from the 1st interface in respect to set and measured, ΔV denotes the normalised CVP with the minimum value 1.88 and maximum value 3.61. In multiple cell experiment, the suspension was not mixed with an agar solution, compared to the single cell as shown in figure 8; therefore, the signal amplitude is larger

Table 1: CVP measured from the agar mock body with three silica sample cells.

$\mathbf{A_z}$ n=1,2,3,4,5,6	$\boldsymbol{X}$ **setting** **(mm)**	X' Measured (mm)	CVP Gain(39)dB **(mV)**	CVP Original **(mV)**	CVP Normalized $(\Delta \boldsymbol{V})$	Standard Deviation
A1	0	0	232.2	2.6	0.58	**3.45%**
A2	10	9.96	193.5	2.17	0.26	**5.05%**
A3	22	21.82	167.7	1.88	0.05	**4.95%**
A4	32	31.80	161.25	1.81	0	**3.12%**
A5	44	42.72	228	2.56	0.55	**6.7%**
A6	54	53.96	322.2	3.61	1	**5.9%**

We repeated the measurements three times for each sample. To calculate the standard deviation of a sample of N=3 measurements, the sum of three measurements divided by N to get the mean value, and then subtract this mean from each measurement to obtain N deviation. The squared N deviation is then divided by (N-1), and the square root taken.

4 Discussion

The ultrasound vibration potential distribution (UVPD) model based on a static charged disc dipole field is proposed. Setting a single and a multiple sample cells are numerically simulated and experimentally measured. The effect of the disc dipole diameter on UVP signal strength is simulated. With an assumption that the ultrasound beam width is the same as the diameter of the ultrasound transducer (in 25 mm), signals from the set-up of the multiple sample cells are simulated and measured as given in Figure 12. To remove the scale effected the data obtained from the simulation and measurement, both sets of data were normalised. The comparison between experimental and simulation measurements as shown in the Figure 12 shows compatible results. The offset appeared at the left side in figure 12 may be due to the effect of earthling points, where only the grounded metal shell of the transducer is considered in the simulation, however, one of the electrode is actually grounded due to the use of a single input of the oscilloscope. Therefore, the measurements close to the nearside are smaller than those from simulation. The different between the first and the second signals mainly due to the electric field attenuation where the sample cells were shifted from the centre of the distance between two electrodes. Therefore, the signals are larger when the distance between electrodes and the sample cells interfaces are smaller and vice versa.

It is also suggested a differential voltage measurement would be preferable, in addition to the ultra-high input impedance, which would be necessary for enhancing the measurement accuracy, particularly from IVP or low concentration colloids. The electrode size is negligible due to the use of voltage measurement, which were experimentally proved. The simulation also indicates the optimized locations of electrodes should be at the nearside and rear-side of the body, although UVP can be measured between anywhere around the body except the locations in orthogonal to the direction of ultrasound propagation, in the principle.

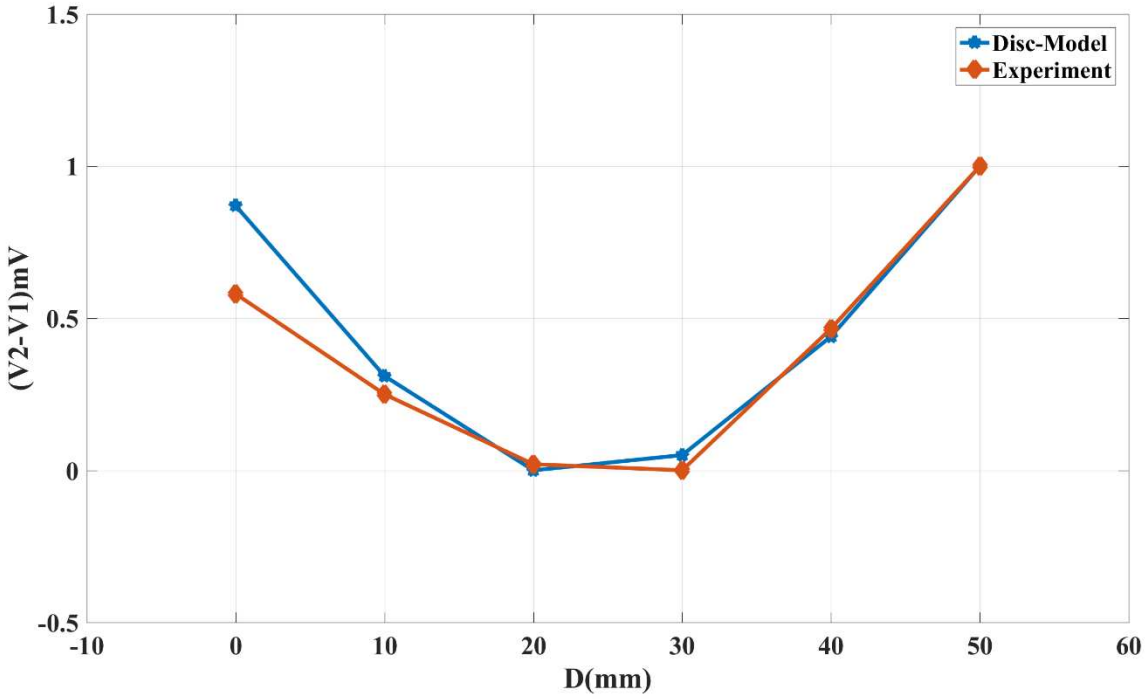

Figure 12: Signal comparison based on data from the simulation and measurement of three sample cells.

The analogue model of ultrasound vibration potential distribution presented between two parallel-grounded electrodes calculated for an infinitive colloidal layer by Cuong et al. [7]. This model is not evaluated experimentally and in this model, the relationship of the measured voltage via integrations is not revealed. However, in our model we introduced a numerical and experimental solution to present the potential distribution for the device optimizations. In the past, two standard devices were not capable of non-intrusive measurement. Here, we established a new testing phantom, which is capable of non-intrusive ultrasound vibration potential measurement and enhance the UVP signal strength.

5 Conclusion

UVP and its distribution UVPD may be concerned as they are generated by a static charged disc dipole located at the interface of a sample cell due to temporal steady state of ultrasound pulses in their propagation cross the interface. Therefore, a static charged disc dipole model is proposed to reveal the ultrasound vibration potential distribution (UVPD) inside a finite region, e.g. in an agar mock body. The simulated UVPD has highest value at the perpendicular plane near the potential reference plane between the two-disc dipole, as well as along the axis of ultrasound propagation. The results also indicate that the UVP is better to be measured between the nearside and rear-side of the phantom and maximum value can be obtained between the two

points along the propagation axial direction. It demonstrates that the ultrasound vibration potential (UVP) signal is measurable in peak-to-peak amplitude of 162/309 μV and 419/499 μV with two electrodes, non-intrusively contacted with the agar mock body containing either ionic electrolyte (1M KCL) and nanoparticle suspension (1%wt of 21nm silica particles) agar gel samples respectively, in a range of 1.8-2.6 mV from sample cells with agar-colloid (1%wt of 21nm silica particle suspension) interfaces arranged along the propagating of ultrasound inside the agar mock body. Further results from both simulated and experimental three cells set-ups have a good agreement, which demonstrates the UVP signal intensity is inversely proportional to the separation distance between the electrodes and the sample cells and evidences the UVP signal attenuation is mainly caused by electric field attenuation. Results conclude the static charged disc dipole model can provide a simple and alternative method to model both ultrasound vibration potential distribution and ultrasound vibration potential measurement.

References

[1]. Debye, P. A Method for the Determination of the Mass of Electrolytic Ions. *Chemical physics.* 1933, **1**(1), pp.13-16.

[2]. Ohshima, H. and Dukhin, A.S. Colloid vibration potential in a concentrated suspension of the spherical colloidal particle. *Journal of Colloid and interface science,.* 1999, **212**(2), pp.449-451.

[3]. Vitalyi , E.G. and Diebold, G., J. Imaging with the ultrasonic vibration potential: A theory for current generation. *Ultrasound in Med. & Bio.* 2005, **31**(2), pp.273-278.

[4]. Khan, J.I., Wang, M., Schlaberg, H.I. and Guan, P. Effect of ion vibration potential for 1-1 electrolytes. *Chemical physics.* 2013, **425**(8), pp.14-18.

[5]. O'Brien, R.W. Electro-acoustic effects in a dilute suspension of spherical particles. *Journal of Fluid Mechanics.* 1988, **190**(-1), p.71.

[6]. Guang, P., Wang, M., Inaki, H.S., Khanj, J.I. and Valerie, S. Towardsd a-scan imaging vibration potential measurement. *Nuclear Engineering and Design.* 2011, **241**(6), pp.1994-1997.

[7]. Cuong, K.N., Vitalyi , E.G. and Diebold, G.J. Potential distribution from electroacoustic polarization sources. *Applied Physics Letter.* 2008, **93**(18), pp.1-3.

[8]. Wang, M., Bramson, L. and Khan , J.I. Methods of Colloid Vibration Imaging for Characterisation of Nano-Particles Suspensions. *NSTI Nanotech.* 2013, **3**, pp.16-19.

[9]. Makino, K. and Ohshima, H. Electrophoretic Mobility of a Colloidal Particle with Constant Surface Charge Density. *Langmuir.* 2010, **26**(23), pp.18016-18019.

[10]. Hossein F, Wang M. Colloid Vibration Potential Imaging for Medicine. J Biomed Imag Bioeng. 2019;3(1):114-118.

[11] Andrew, C.B., Wang, S. and Diebold, G.J., Imaging based on the ultrasonic vibration potential. *Applied Physics Letter.*2004, 85(22), pp.5466-5468.

[12] Adam D. Maxwell, Tzu-Yin Wang, Lingqian Yuan, Alexander P. Duryea, Zhen Xu, and Charles A. Cain, A tissue phantom for visualization and measurement of ultrasound-induced cavitation damage, *Ultrasound Med Biol.* 2010, 36(12), pp.2132–2143

Contents